Electronic Supplementary Material (ESI) for Physical Chemistry Chemical Physics.

Supporting Information:

Mechanism of monolayer to bilayer silicene transformation in $CaSi_2$ due to fluorine diffusion

Akihiro Nagoya, Ritsuko Yaokawa, & Nobuko Ohba

S1. HAADF-STEM observations of F agglomerated areas in $CaSi_2$

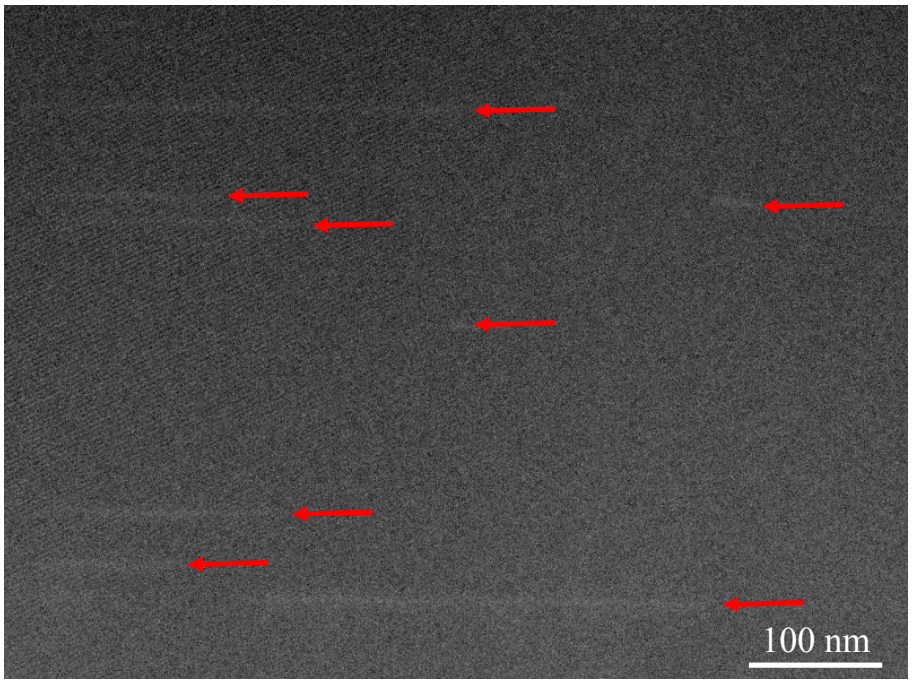

Fig. S1 Low-magnification HAADF–STEM image of area 1 from Fig. 1 (c), with the bright-contrast lines indicated by red arrows.

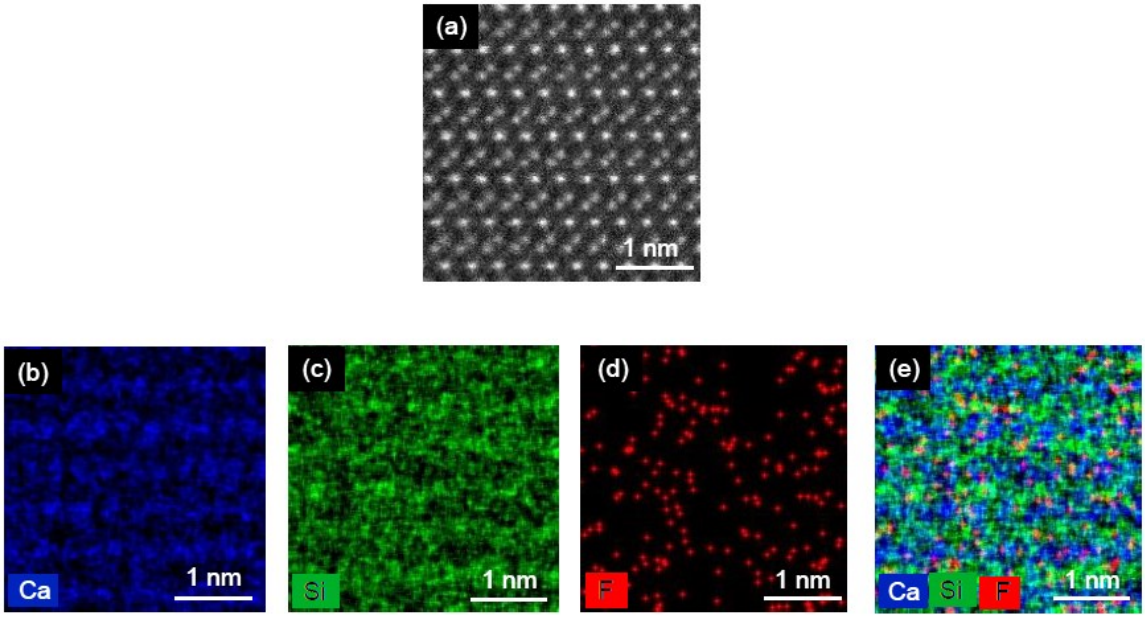

Fig. S2 (a) Atomic-resolution HAADF–STEM image of the $CaSi_2$ parent phase that appeared as dark contrast in the area of low fluorine concentration (i.e., area 1) of Fig. 1 (c). (b–d) STEM–EDX elemental mappings of (b) Ca, (c) Si, and (d) F. (e) STEM–EDX overlapped mapping of Ca, Si, and F.

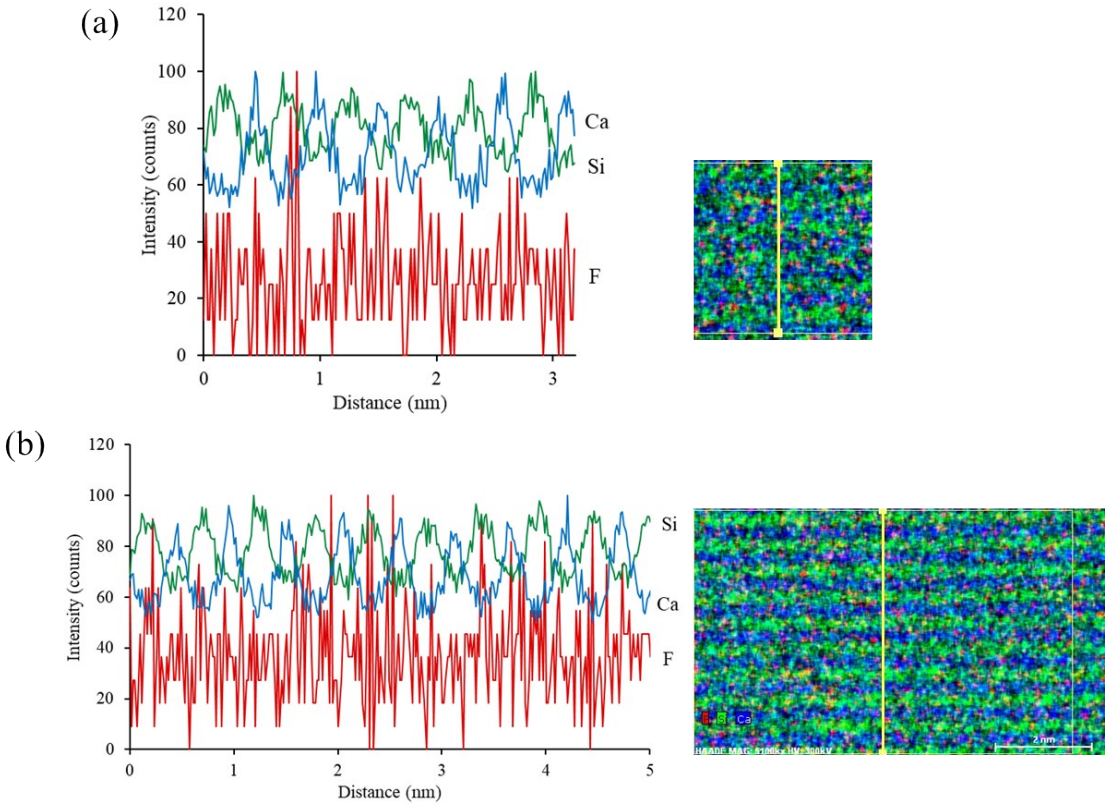

Fig. S3 EDX line profiles of Ca, Si, and F, and analysis locations in the EDX mappings for (a) Fig. S2(e) and (b) Fig. 2(c), with detection intensity determined as the sum along a line 0.6 nm wide (yellow line).

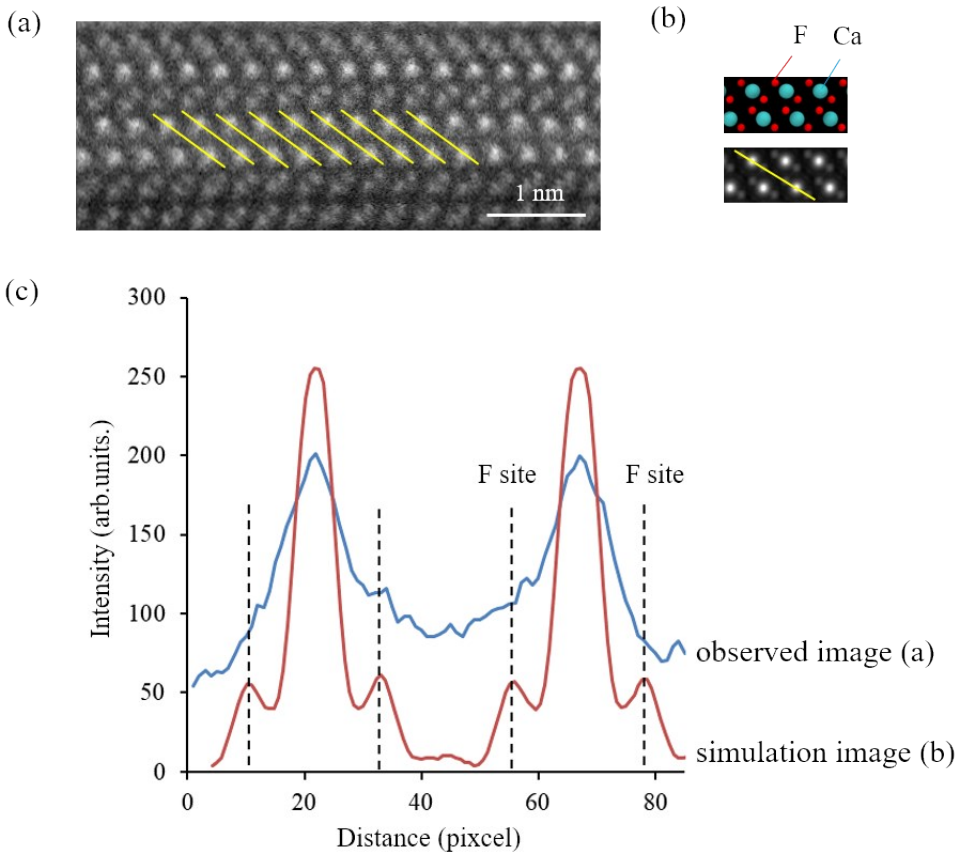

Fig. S4 (a) HAADF–STEM image of CaF_x layer in area 3 of Fig. 4(a), with (b) the CaF_2 crystalline model along the [−110] incident direction and the HAADF–STEM simulation image (MacTempasX; multi-slice method). (c) Average line profiles of CaF_x layer in (a) and of simulation image in (b), with F atoms occupying only the F sites between the Ca layers.

S2. F atom diffusion barriers in $CaSi_2$

S2.1 Intra- and interlayer diffusion

Diffusion barriers (ΔG) for the F atoms in $CaSi_2$ were calculated (Fig. S5). More specifically, diffusion barriers related to F diffusion to adjacent Ca_3 center sites in the initial state (IS) and final state (FS) were calculated based on the Climbing Image Nudged Elastic Band (CI-NEB) model[1,2]. Intralayer diffusion in the Ca layer and interlayer diffusion to other Ca layers were calculated. Interlayer diffusion pathways were based on a pathway that diffused along the translational direction to the *c*-axis of the hexagonal crystal. Energy barriers for intralayer diffusion and interlayer diffusion were 1.3 and 2.5 eV, respectively (Fig. S5). Reaction rate constants (k) were calculated at the temperature T=600 K based on state transition theory as

$$k = \frac{k_B T}{h} \exp\left(-\Delta G / k_B T\right), \quad \text{(S1)}$$

where k_B and h are the Boltzmann constant and the Planck constant, respectively. The k values for intralayer and interlayer diffusion were 10 and 0.01 s^{-1}, respectively. Therefore, intralayer diffusion was favored compared to interlayer diffusion.

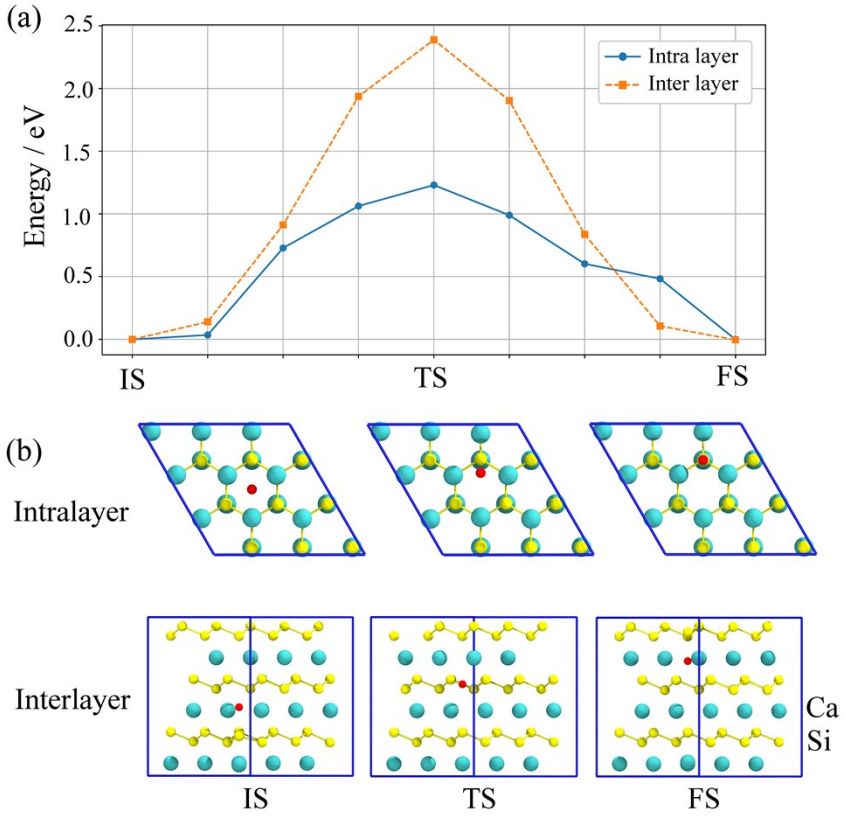

Fig. S5 (a) Diffusion barriers for interstitial F atoms in 3R-$CaSi_2$ and (b) structures in the Initial State (IS), Transition State (TS), and Final State (FS).

S3. Interstitial sites of F atoms in $CaSi_2$

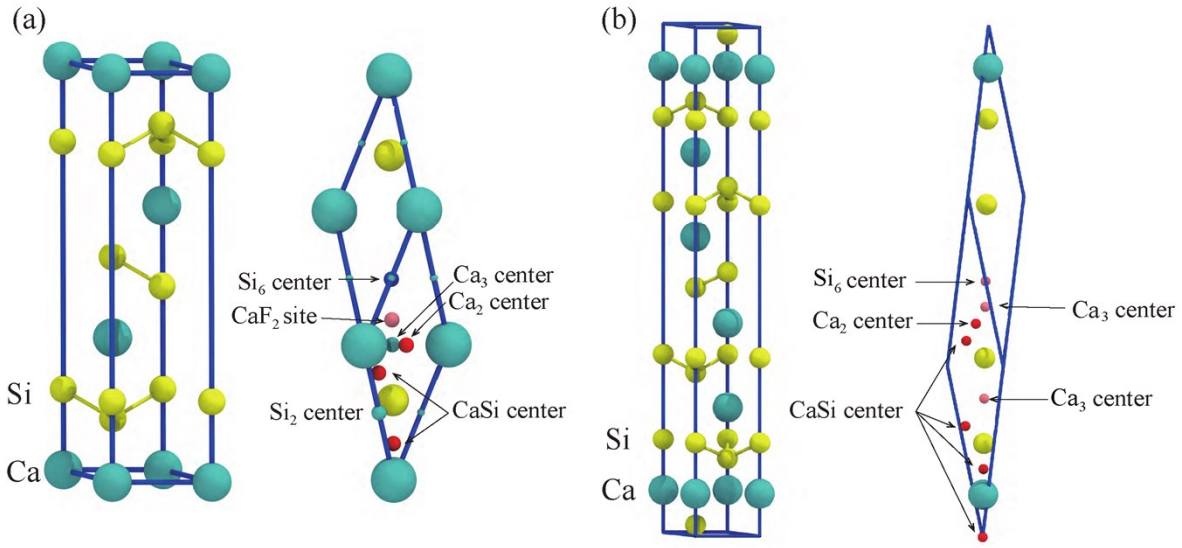

Fig. S6 Crystal structure of $CaSi_2$ represented as (a) 3R and (b) 6R structures, shown as hexagonal and rhombohedral unit cells. The rhombohedral unit cell includes the calculated interstitial sites for F atoms as indicated by dots of various colors.

Table S1 Formation energy (ΔG^f) for interstitial F atoms in $CaSi_2$, using the Ca_3 center of lowest formation energy as the baseline. The results for two inequivalent sites of Ca_3 centers are shown for 6R structure.

	ΔG^f / eV	
Site	**3R**	**6R**
Ca_3 center	0.00	0.37, 0.00
Ca_2 center	0.62	2.05
Si_6 center	2.89	2.77
CaSi center	3.51	3.19

S3.1 First-principles molecular dynamics method for $CaSi_2F$

Ab initio molecular dynamics (AIMD) simulation of $CaSi_2F$(P21/m) was conducted using a supercell composed of 384 atoms at a temperature of 800 K and a pressure of 1 atm. The cutoff of the plane waves was 400 eV, and the k-point was the Γ point. The number of atoms N, temperature T and pressure p were kept constant based on an (N, p, T) ensemble with a Langevin thermostat and a Parrinello–Rahman barostat [3,4]. The lattice and atomic friction coefficients were set to the values used in the literature for the calculations of Me_3AlF_6[7](Me = Li, Na, K, Rb), with 10 ps^{-1} and 2 ps^{-1}

respectively applied as relevant timeframes[5,6]. Despite previous reports recommending the application of 2 amu as the lattice mass, the calculation became unstable at this lattice mass, so a larger value of 10 amu was used instead.

The initial and final structures are shown in Figs. S7(a) and (b). The buckled honeycomb lattice of Si atoms was largely disordered. Some sections of the Si layer formed a square lattice, while other sections consisted of disorderly arrays with four- and five-membered rings. Square lattices were observed adjacent to the CaF domain, where the Ca–Ca distance was shorter than in the initial structure, while disorderly arrangements were observed at domain interfaces. The lattice vector along the atomic layer became shorter, while the lattice vector perpendicular to the atomic layer became longer. The square lattice of Si and CaF domains formed a ZrCuSiAs structure belonging to the P4/nmm space group.

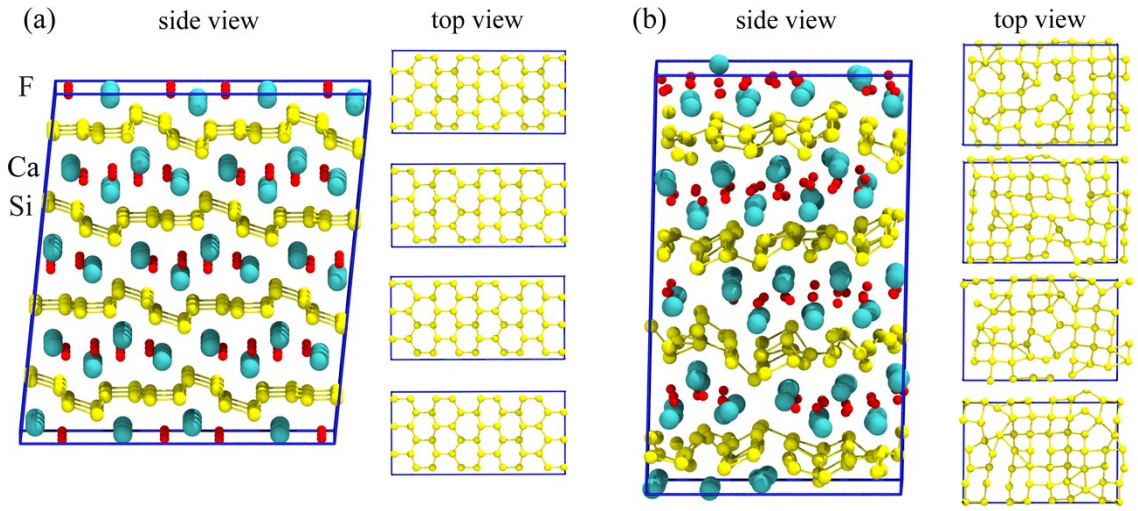

Fig. S7 AIDM calculations of (a) initial structure and (b) structure after treatment at 800 K for 30 ps, showing top views of each of the four Si atomic layers in the unit cell.

References

1 G. Henkelman, B.P. Uberuaga, H. Jónsson, *J. Chem. Phys.* 2000, **113**(22), 9901–9904.

2 G. Henkelman, B. H. Jónsson, *J. Chem. Phys.* 2000, **113**(22), 9978–9985.

3 M. Parrinello, A. Rahman, *Phys. Rev. Lett.* 1980, **45**(14), 1196.

4 M. Parrinello, A. Rahman, *J. Appl. Phys.* 1981, **52**(12), 7182–7190.

5 T. Bučko, F. Šimko, *J. Chem. Phys.* 2016, **144**(6), 064502.

6 T. Bučko, F. Šimko, *J. Chem. Phys.* 2018, **148**(6), 064501.